Research Article Open Access

Sezer Erdem*, Beyhan Erdem, Ramis Mustafa Öksüzoğlu

Magnetic Nano-Sized Solid Acid Catalyst Bearing Sulfonic Acid Groups for Biodiesel Synthesis

https://doi.org/10.1515/chem-2018-0092
received January 30, 2018; accepted May 4, 2018.

Abstract: In our approach for magnetic iron oxide nanoparticles surface modification, the fabrication of an inorganic shell, consisting of silica by the deposition of preformed colloids onto the nanoparticle surface and functionalization of these particles, was realized. The magnetic nanoparticles, non-coated and coated with silica layer by Stöber method, are functionalized with chlorosulfonic acid. The magnetic nanoparticles (MNPs), in size of 10-13 nm, could be used as acid catalyst in biodiesel production and show superparamagnetic character. The prepared nanoparticles were characterized by different methods including XRD, EDX, FT-IR and VSM. The catalytic activity of the coated and non-coated solid acids was examined in palmitic acid-methanol esterification as an industrial reaction for biodiesel synthesis. Although thin silica layer results in only a minor obstacle with respect to magnetism, it can accelerate the mass transportation due to its relatively porous structure and magnetic core may be more stable in the acidic reaction medium by means of covering process. Accordingly, coating strategy can be efficient way for allowing applications of MNPs in acid catalyzed esterification.

Keywords: Magnetic Nanoparticles; Solid Acid Catalyst; Biodiesel Synthesis; Sulfonic Acid; Esterification.

PACS: 75.75.Cd, 88.20.fk

1 Introduction

Rising demand for energy and fuel, row oil reserves crisis and environmental regulations have augmented the interest in biodiesel as a renewable and greener option to diesel based on petroleum [1]. Biodiesel consists of long chain fatty acid esters produced with esterification of free fatty acids with methanol/ethanol or transesterification of triglycerides. In addition to being a renewable resource, biodiesel has many advantages such as a higher flash point, increased lubricity, and a lower emission profile compared with conventional diesel. Also, biodiesel is non-toxic and biocompatible. Because of these attractive properties, biodiesel is a fully environmentally friendly fuel [2].

Despite the currently usage of homogeneous catalytic process for the industrial production of biodiesel, it suffers many drawbacks such as difficulty in separation and the need to deal with the corrosive waste containing acid. Due to the ability to moderate high-acid value of oils as feedstock, heterogeneous acid catalysts are particularly attractive candidates for the biodiesel production process. Therefore, the appropriate heterogeneous solid catalysts for biodiesel production would have a growing interest [3].

Many heterogeneous acid catalysts such as zeolite, ion-exchange resin activated by sulfonation, and sulfated zirconia have been used for acid catalyzed reactions. However, catalysts such as zeolites have micropores and these micropores prevent the diffusion of big reaction components having long alkyl chains. For this reason, zeolites are not recommended for biodiesel synthesis. Ion-exchange resins are active strong acids. However, they have low thermal stability and deactivation takes place after only 2-5 hours. Since the stability of catalyst is decreased by the hindering of the smaller pores which are than the reaction components and coke formation, sulfated zirconia also is not appropriate [4]. Because of the low acid loading or the diffusional limitations of porous materials, the current solid acid catalysts show low activity. Due to these reasons, we choose magnetic nanoparticles (MNPs) as the carriers to prepare nano-size solid catalyst containing sulfonic acid groups on the surface. Nanoparticles as heterogeneous catalyst supports have attracted increasing interest, because the particles in nanometer size have large surface area, which provides quite several active and accessible centers. Furthermore, MNPs provide an additional

***Corresponding author: Sezer Erdem,** Uludag University, Physics Department, Bursa, Turkey, E-mail: serdem@uludag.edu.tr
Beyhan Erdem: Uludag University, Chemistry Department, Bursa, Turkey
Ramis Mustafa Öksüzoğlu: Anadolu University, Material Science and Engineering Department, Eskisehir, Turkey

advantage in separation and filtration steps for recycling tests [5]. Surface modification of magnetic particles is an elegant way to build a bridge between homogeneous and heterogeneous catalysis. In many organic reactions, silica-coated and sulfuric acid functionalized MNPs as recyclable strong solid acid catalysts facilitate the recovery of the catalyst [6]. MNPs of an ideal size are applied in the form of a stable aqueous suspension, and they should have superparamagnetic character. Superparamagnetism is a phenomenon whereby the magnetic moments of nanoparticles are smaller than a particular thermal energy. Since the particles have almost no coercivity, there are no magnetic interactions between them, which lead to the aggregation of the superparamagnetic nanoparticles. On the contrary, the magnetic interactions between larger particles named as ferri/ferromagnetic prevent to obtain a stable suspension [7].

Successful applications of MNPs highly depend upon their state of being stable especially under low pH conditions. According to previous studies [8], it is beneficial to use silica coated MNPs to ensure that they are stabilized. The silica layer acts both as a protective layer and scaffold, which makes functionalization possible by means of surface hydroxyl groups. While a thick silica layer would be useful to keep the distances between the core and the surface, it should also be thin enough to maintain the magnetic properties [9].

In the esterification reactions catalyzed by solid acid catalysts, the water, one of the reaction products, not only poisons the surface of the catalyst, but also produces more hydrophilic environment, reducing the performance of the solid acid catalyst. In addition to poisoning of the catalyst's surface in the presence of water molecules, the active acidic sites of the catalysts are also exposed to deactivation, which inhibits the progress of the reactions. Apart from these, there are important parameters affecting the reactions' progress considerably such as the polarities of the reactants and products, hydrophobic-hydrophilic balance on catalyst's surface, and the acidity of catalysts [10].

The goal of this work is to increase the chemical stability of the sulfonic acid functionalized MNPs catalysts at low pH media by coating silica on the surface of MNPs before functionalization with sulfonic acid. At first, Fe_3O_4 nanoparticles are synthesized by co-precipitation of Fe^{2+} and Fe^{3+} salt solutions. Then, MNPs are coated with silica layer by Stöber method. Subsequently, the non-coated and coated MNPs are functionalized with chlorosulfonic acid. The catalytic activity of the coated and non-coated solid acids was examined in the palmitic acid-methanol esterification as an industrial reaction for biodiesel synthesis.

2 Experimental

2.1 Chemicals and Instruments

All chemicals were acquired from Merck or Sigma Aldrich and used as received. The X-ray diffraction patterns were recorded between 10° and 80° (2θ) in a Rigaku-Rint 2200 X-ray diffractometer (XRD) with CuK_α radiation (λ = 0.154 nm). FT-IR measurements were performed by using a Perkin Elmer-UATR Two series infrared spectrometer. The components of the nanoparticles were analyzed by using energy dispersed X-ray spectrometer (EDX, Quanta-Bruker AXS). Magnetic properties were examined at room temperature by using a vibrating sample magnetometer (VSM, X9 Microsense) with a maximum applied field of 20 kOe.

2.2 Preparation of the Magnetic Fe_3O_4 Nanoparticles (MNPs)

MNPs were synthesized by chemical co-precipitation method described in the literature [11]. In a typical synthesis, $FeCl_3.6H_2O$ (0.0216 mol) and $FeCl_2.4H_2O$ (0.0108 mol) were dissolved in 100 mL deionized water at 85°C under N_2 atmosphere with vigorous stirring. NH_4OH, after being added as base to the Fe^{2+} and Fe^{3+} salt solutions, the black precipitate was magnetically separated.

2.3 Preparation of MNPs Coated by Silica

$Fe_3O_4.SiO_2$ nanoparticles were prepared according to the reported method [12]. MNPs (1 g) were firstly dispersed in the mixture of water (20 mL), ethanol (60 mL), and concentrated NH_4OH (2 mL, 25 wt%) and then homogenized by ultrasonic. A solution of TEOS in ethanol (1 mL/10 mL) was dropped into the dispersion under mechanical stirring. The product, $Fe_3O_4.SiO_2$, was separated by a magnet.

2.4 Preparation of Sulfonic Acid Functionalized Magnetic Nanoparticles

Naked Fe_3O_4 and $Fe_3O_4.SiO_2$ samples were ultrasonically dispersed in dry CH_2Cl_2. Consecutively, chlorosulfonic acid (1 mL) was dropped into the dispersion, which was put in the cooled ice bath within 30 min, accompanied by HCl gas evolving from the reaction vessel. The resulting materials ($Fe_3O_4.SO_3H$ and $Fe_3O_4.SiO_2.SO_3H$) were separated with the

help of magnet and washed with dry CH_2Cl_2 and ethanol to eliminate the hardly attached substrates as mentioned by Safari and Zarnegar [6].

2.5 General Procedure for the Esterification of Palmitic Acid with Methanol

Palmitic acid-methanol esterification was carried out in an isothermal glass reactor as mentioned in the literature [13]. In a typical run, 1.75 g of palmitic acid was charged into the 100 mL reactor equipped with a heating jacket and a temperature control unit with an accuracy of ± 0.1°C, and 31.8 mL of methanol was added. The necessary amount of the solid acid catalyst was taken into the reaction mixture accompanied by refluxing and stirring. The liquid samples (0.5 mL), withdrawn from the reactor at regular intervals, were analyzed volumetrically after being dispersed in ethanol/diethyl ether mixture. A 0.01 N alkaline solution of KOH was used to perform titration. The percentage of palmitic acid conversion (X_A%) was calculated [14].

The acidity of the catalysts was estimated by ion-exchange analysis. The catalyst (0.05 g) was added to NaCl (2M, 15 mL) aqueous solution and stirred for 1 day. Then, the resulting mixture was titrated by NaOH (0.05 M).

Ethical approval: The conducted research is not related to either human or animals use.

3 Results and Discussion

The diffractograms of naked (Fe_3O_4) and covered with silica layer ($Fe_3O_4.SiO_2$) samples are shown in Figure 1a. The observed XRD patterns appearing at 2θ = 30.5°, 35.8°, 43.4°, 53.9°, 57.3°, 63.1°, 71.7° and 74.8° and corresponding Miller indices values {hkl} of (220), (311), (400), (422), (511), (440), (620), and (533) reveal cubic iron oxide phase with the structure of inverse spinel ferrite of magnetite (JCPDS file no. 19-0629) [15]. The broad peak (2θ = 18-25°) in the $Fe_3O_4.SiO_2$ sample could be attributed to the amorphous silica in the form of a shell over the Fe_3O_4 core and this result is in good agreement with that of Mobaraki et al [10]. The mean particle-size of Fe_3O_4 and $Fe_3O_4.SiO_2$ samples was calculated by Scherrer's equation [16], D = k λ / β Cos θ, resulting in 12.6 nm and 14.2 nm for the Fe_3O_4 and $Fe_3O_4.SiO_2$ samples, respectively (Table 1). Figure 1b shows the XRD diffraction patterns of sulfonic acid functionalized Fe_3O_4 and $Fe_3O_4.SiO_2$ samples. The position and relative intensities of all XRD patterns match well with the peaks of the samples shown in Figure 1a,

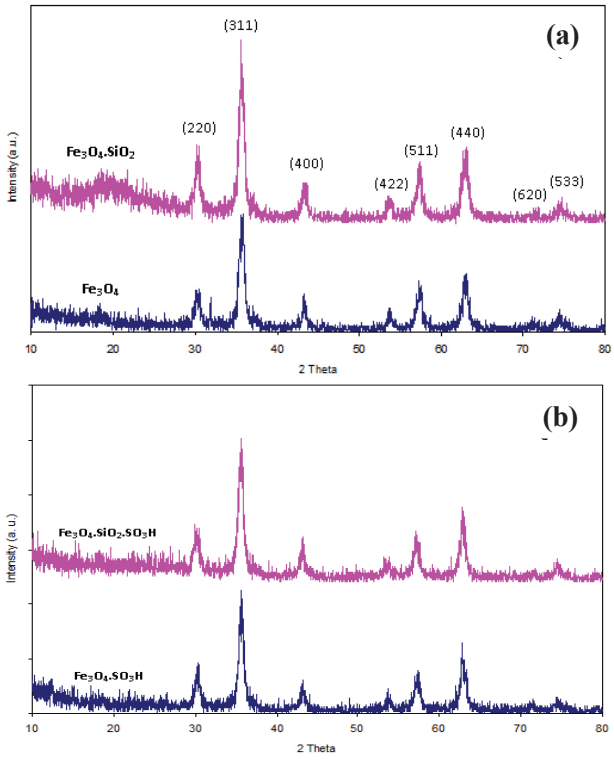

Figure 1: XRD patterns of Fe_3O_4 and $Fe_3O_4.SiO_2$ (a); $Fe_3O_4.SO_3H$ and $Fe_3O_4.SiO_2.SO_3H$ (b).

indicating the maintenance of the crystalline structure. Consequently, it can be concluded that the frameworks of the $Fe_3O_4.SO_3H$ and $Fe_3O_4.SiO_2.SO_3H$ samples remained unchanged [17].

Figure 2a shows the FT-IR spectra of the uncoated (Fe_3O_4) and coated ($Fe_3O_4.SiO_2$) MNPs. In the spectrum of Fe_3O_4 MNPs, absorption peaks at 544, 3419 and 1627 cm^{-1} correspond to the Fe-O and O-H stretching vibrations, and to the O-H bending vibration, respectively. The characteristic absorption peaks for the silica network are in accordance with the literature [18]. The broad and high-intensity band at 1077 cm^{-1} is assigned to the asymmetric stretching of Si-O-Si in SiO_4, the band at 797 cm^{-1} is due to the Si-O-Si symmetric stretching, and the formation of the peak around 450 cm^{-1} is most likely attributed to the Si-O-Si bending mode. The weak band at 950 cm^{-1}, which was absent in Fe_3O_4, is due to the Si-OH deformation from the incomplete condensation of TEOS sol [19]. Another FT-IR analysis showed the presence of the $-SO_3H$ groups attached to the surface of the MNPs (Figure 2b). As shown in Figure 2b, the FT-IR spectrum of $Fe_3O_4.SO_3H$ was definitely different from that of Fe_3O_4 in Figure 2a. The broad band between 3500 and 3000 cm^{-1} was attributed to adsorbed water and the broad band in range of 1200-1050 cm^{-1} was

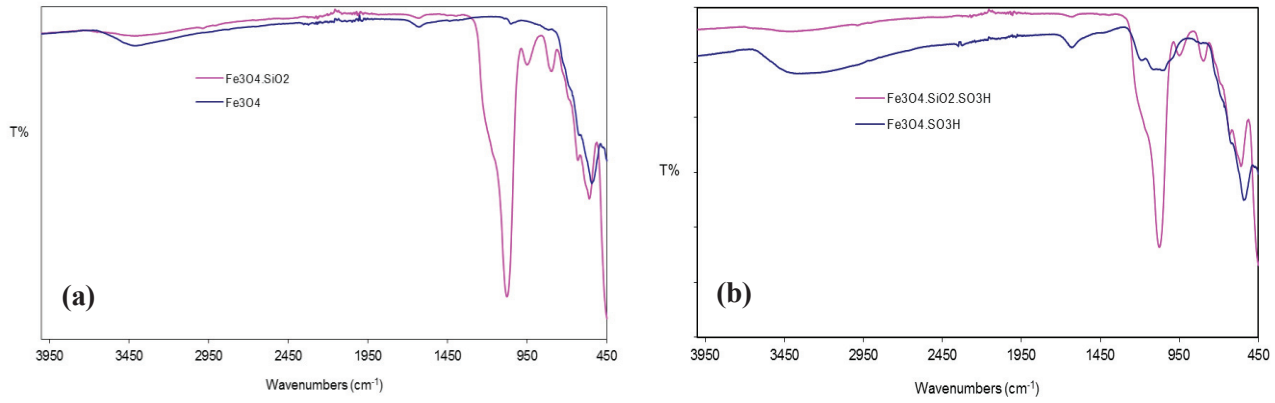

Figure 2: The comparative FT-IR spectra (a) for Fe_3O_4 and $Fe_3O_4.SiO_2$; (b) $Fe_3O_4.SO_3H$ and $Fe_3O_4.SiO_2.SO_3H$ samples.

attributed to the symmetric SO_2 stretching indicating the presence of SO_3H groups [20]. According to the literature [21], the peaks at 1199 and 1129 cm^{-1} confirmed the presence of S=O group. In our $Fe_3O_4.SO_3H$ sample, these peaks were observed at 1194 and 1115 cm^{-1} demonstrating the presence of SO_3H groups. On the other hand, these bands were covered by stronger absorption of the Si-O band at 1077 cm^{-1} for the $Fe_3O_4.SiO_2.SO_3H$ sample. All these observations confirm that the sulfonyl groups have functionalized both of the surfaces of Fe_3O_4 and $Fe_3O_4.SiO_2$ samples.

In order to improve the surface reactivity of MNPs, coating by silica is recommended because of the silanol groups (Si-OH) which can be functionalized by further treatment. Therefore the surface concentration of the –OH groups may be correlated with surface density of the Si atoms [22]. For this purpose, the components of $Fe_3O_4.SiO_2$, $Fe_3O_4.SO_3H$ and $Fe_3O_4.SiO_2.SO_3H$ samples were determined by using EDX as illustrated in Figure 3. According to EDX results, Fe_3O_4 nanoparticles were trapped by SiO_2 in $Fe_3O_4.SiO_2$ sample. The characteristic peaks of Sulphur (S) in $Fe_3O_4.SO_3H$ and $Fe_3O_4.SiO_2.SO_3H$ proved that sulfonyl groups were successfully attached onto the surface of both nanoparticles.

Figure 4a shows the M-H hysteresis curves of Fe_3O_4 and $Fe_3O_4.SiO_2$ nanoparticles. The saturation magnetization (M_s) of the silica coated MNPs represents the magnetic content of 84% of Fe_3O_4. M-H hysteresis curves (Figure 4a, b) have a negligible coercivity and remanence. In addition, the increasing magnetization with the external magnetic field could not reach saturation even at 20 kOe. All of these features arise from superparamagnetic character of the nanoparticles [23]. The small decrease (16%) in the M_s value can be attributed to thin silica layer (Table 1). The M_s value of the $Fe_3O_4.SO_3H$ and $Fe_3O_4.SiO_2.SO_3H$ samples obtained from the M-H curves shown in Figure 4b are 52.6

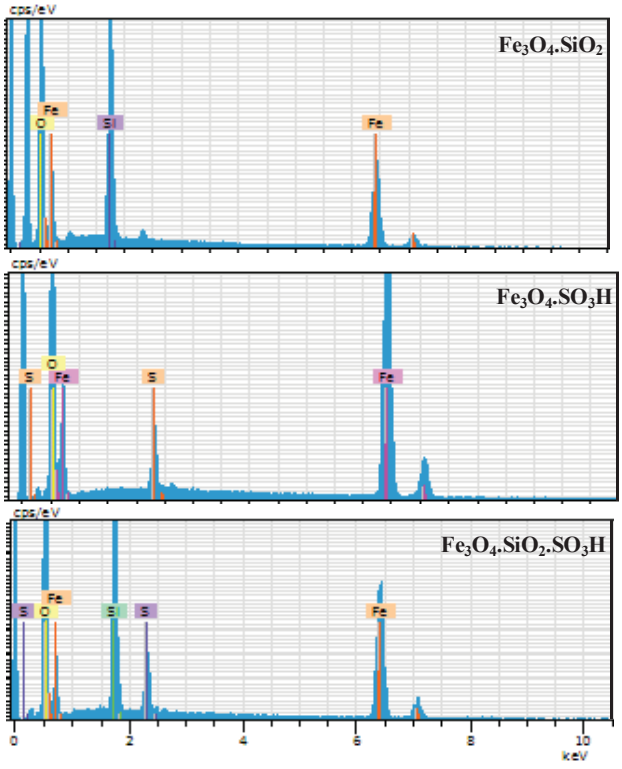

Figure 3: The EDX spectra of $Fe_3O_4.SiO_2$, $Fe_3O_4.SO_3H$ and $Fe_3O_4.SiO_2.SO_3H$ nanoparticles.

and 41.1 emu g^{-1}, respectively. These values are smaller in comparison to those of the Fe_3O_4 and $Fe_3O_4.SiO_2$ samples, namely, by a factor of about 21%. These results reflect that sulfonic acid functionalization causes the decrease of magnetization. It was also confirmed that the single domain magnetic nanoparticles existed yet already in these acid catalysts [24]. According to mean particle sizes given in Table 1, the larger nanoparticles having higher

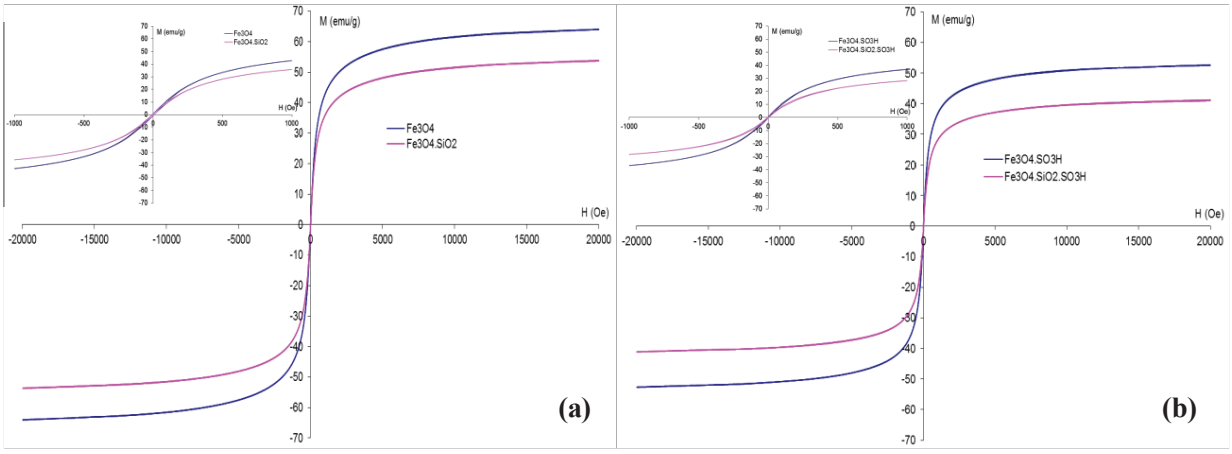

Figure 4: M-H hysteresis curves for the Fe_3O_4 and Fe_3O_4.SiO_2 (a), Fe_3O_4.SO_3H and Fe_3O_4.SiO_2.SO_3H samples (b) at room temperature (-1000 and 1000 Oe inset).

Table 1: Saturation magnetization values based on VSM data and mean particle sizes calculated by XRD.

	Saturation Magnetization (emu/g)	Mean Particle Size (nm)
Fe_3O_4	64.0	12.6
Fe_3O_4.SiO_2	53.7	14.2
Fe_3O_4.SO_3H	52.6	12.9
Fe_3O_4.SiO_2.SO_3H	41.1	13.3

magnetizations were initially sedimented, resulting in a decrease in the mean size of the nanoparticles. Even with this reduction in the M_s values, the catalysts can still be efficiently and easily separated from solution by using an external magnetic force and M_s values obtained in this study are also consistent with the reported values in the literature [25,26].

According to the expression, $D_{mag}=\left(\frac{18kT(dM/dH)_0}{\pi\rho M_s^2}\right)^{1/3}$ the size of the superparamagnetic MNPs was calculated by using the slope of the hysteresis curve near H=0 [27]. Taking the M_s value obtained from M-H curve, the size of Fe_3O_4 was estimated as 10.6 nm which is smaller than that of XRD result (12.6 nm). The experimental error in the extrapolated M_s value and the magnetite density may have contributed to the discrepancy except the contribution of true phase composition [27].

Chlorosulfonic acid, which is used as an acid precursor for functionalizing, provides the acid sites for the Fe_3O_4 and Fe_3O_4.SiO_2 supports and the self-condensation of chlorosulfonic acid was verified by the yield of the solid acid catalyst. Increasing the amount of the precursor provides the effective density of acid sites. However, the use of excess chlorosulfonic acid may corrode the magnetic core due to the acid-base neutralization reactions. Although a high acidity was obtained for the Fe_3O_4.SO_3H (5.1 mmol g^{-1} with ± 2.9%) compared to the Fe_3O_4.SiO_2.SO_3H (4.1 mmol g^{-1} with ± 2.9%), the catalytic activity of the Fe_3O_4.SiO_2.SO_3H is higher than that of the Fe_3O_4.SO_3H (Figure 5). According to experimental results, the Fe_3O_4.SiO_2.SO_3H was obtained with a solid yield of 75% and the Fe_3O_4.SO_3H with 59.5% which promotes the idea that magnetic core might have been corroded by the chlorosulfonic acid precursor [28]. Esterification of methyl palmitate is a reversible reaction from which the water is arising as byproduct and the higher acid sites belonging to the Fe_3O_4.SO_3H sample also promoted the reverse reactions causing a longer reaction time compared to Fe_3O_4.SiO_2.SO_3H. Even if the silica covering leads only a little barrier for protecting the MNPs, it can decelerate the mass transport resistance due to its relatively porous structure and magnetic core may be more stable in the low pH medium by means of the covering process.

4 Conclusion

The aim of this study was to synthesize non-coated and silica coated magnetic nanoparticles with activated chlorosulfonic acid, which could be used as catalysts in the esterification and could be separated from reaction medium and collected by magnetic force without centrifugation or filtration. According to the XRD and VSM results, it was concluded that the materials are nano-sized and coated with silica. FT-IR and EDX results confirmed the presence of acid functional groups (-SO_3H).

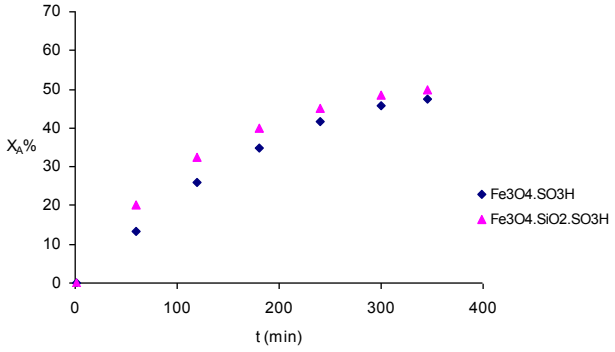

Figure 5: Conversion of palmitic acid as a function of time. Reaction conditions: Palmitic acid: methanol = 1:33 (w/w), 60°C, 3 wt% catalyst.

Though both of $Fe_3O_4.SO_3H$ and $Fe_3O_4.SiO_2.SO_3H$ catalysts efficiently catalyzed the esterification of methylpalmitate, silica coating can accelerate the mass transportation due to its relatively porous structure and magnetic core may be more stable in the acidic reaction medium. In conclusion, low mass transfer resistance, stability, magnetic responsibility, and high reaction efficiency causes the preference of the $Fe_3O_4.SiO_2.SO_3H$ catalyst.

Acknowledgment: This work was supported by The Commission of Scientific Research Projects of Uludag University, Project number: KUAP(F)-2014/33.

Conflict of interest: Authors state no conflict of interest.

References

[1] Zillillah, Tan G., Li Z., Highly active, stable, and recyclable magnetic nano-size solid acid catalysts: efficient esterification of free fatty acid in grease to produce biodiesel, Green Chem., 2012, 14, 3077-3086.
[2] Wang H., Covarrubias J., Prock H., Wu X., Wang D., Bossmann S.H., Acid-Functionalized Magnetic Nanoparticle as Heterogeneous Catalysts for Biodiesel Synthesis, J. Phys. Chem. C, 2015, 119, 26020-26028.
[3] Dang T.H., Chen B.H., Optimization in esterification of palmitic acid with excess methanol by solid acid catalyst, Fuel Process. Technol., 2013, 109, 7-12.
[4] Poonjarernsilp C., Sano N., Tamon H., Hydrothermally sulfonated single-walled carbon nanohorns for use as solid catalysts in biodiesel production by esterification of palmitic acid, Appl. Catal. B Environ., 2014, 147, 726-732.
[5] Wang P., Kong A.G., Wang W.J., Zhu H.Y., Shan Y.K., Facile Preparation of Ionic Liquid Functionalized Magnetic Nano-Solid Acid Catalysts for Acetalization Reaction, Catal. Lett., 2010, 135, 159-164.
[6] Safari J., Zarnegar Z., A magnetic nanoparticle-supported sulfuric acid as a highly efficient and reusable catalyst for rapid synthesis of amidoalkyl naphthols, J. Mol. Catal. A: Chem., 2013, 379, 269-276.
[7] Kralj S., Makovec D., Campelj S., Drofenik M., Producing ultra-thin silica coatings on iron-oxide nanoparticles to improve their surface reactivity, J. Magn. Magn. Mater., 2010, 322, 1847-1853.
[8] Kuzminska M., Carlier N., Backov R., Gaigneaux E.M., Magnetic nanoparticles: Improving chemical stability via silica coating and organic grafting with silanes for acidic media catalytic reactions, Appl. Catal. A: Gen., 2015, 505, 200-212.
[9] Narita A., Naka K., Chujo Y., Facile control of silica shell layer thickness on hydrophilic iron oxide nanoparticles via reverse micelle method, Colloids Surf. A: Physicochem. Eng. Asp., 2009, 336, 46-56.
[10] Mobaraki A., Movassagh B., Karimi B., Hydrophobicity-enhanced magnetic solid sulfonic acid: A simple approach to improve the mass transfer of reaction partners on the surface of the heterogeneous catalyst in water-generating reactions, Appl. Catal. A: Gen., 2014, 472, 123-133.
[11] Kassaee M.Z., Masrouri H., Mohavedi F., Sulfamic acid-functionalized magnetic Fe_3O_4 nanoparticles as an efficient and reusable catalyst for one-pot synthesis of α–amino nitriles in water, Appl. Catal. A: Gen., 2011, 395, 28-33.
[12] Yang D., Hu J., Fu S., Controlled Synthesis of Magnetite-Silica Nanocomposites via a Seeded Sol-Gel Approach, J. Phys. Chem. C, 2009, 113, 7646-7651.
[13] Ramu S., Lingaiah N., Prabhavathi Devi B.L.A., Prasad R.B.N., Suryanarayana I., Sai Prasad P.S., Esterification of palmitic acid with methanol over tungsten oxide supported on zirconia solid acid catalysts: effect of method of preparation of the catalyst on its structural stability and reactivity, Appl. Catal. A: Gen., 2004, 276, 163-168.
[14] Marchetti J.M., Errazu A.F., Comparison of different heterogeneous catalysts and different alcohols for the esterification reaction of oleic acid, Fuel, 2008, 87, 3477-3480.
[15] Bayat A., Shakourian-Fard M., Ehyaei N., Hashemi M.M., A magnetic supported iron complex for selective oxidation of sulfides to sulfoxides using 30% hydrogen peroxide at room temperature, RSC Adv., 2014, 4, 44274-44281.
[16] Naeimi H., Nazifi Z.S., A highly efficient nano-Fe_3O_4 encapsulated-silica particles bearing sulfonic acid groups as a solid acid catalyst for synthesis of 1,8-dioxo-octahydroxanthene derivatives, J. Nanopart. Res., 2013, 15, 2026-2036.
[17] Naeimi H., Nazifi Z.S., Amininezhad S.M., Preparation of Fe_3O_4 encapsulated-silica sulfonic acid nanoparticles and study of their in vitro antimicrobial activity, J. Photochem. Photobiol. B: Biol., 2015, 149, 180-188.
[18] Du G.H., Liu Z.L., Xia X., Chu Q., Zhang S.M., Characterization and application of Fe_3O_4/SiO_2 nanocomposites, J. Sol-Gel Sci. Techn., 2006, 39, 285-291.
[19] Li Y.S., Church J.S., Woodhead A.L., Moussa F., Preparation and characterization of silica coated iron oxide magnetic nano-particles, Spectrochim. Acta Part A: Mol. Biomol. Spectrosc., 2010, 76, 484-489.

[20] Nemati F., Heravi M.M., Rad R.S., Nano-Fe_3O_4 Encapsulated-Silica Particles Bearing Sulfonic Acid Groups as a Magnetically Separable Catalyst for Highly Efficient Knoevenagel Condensation and Michael Addition Reactions of Aromatic Aldehydes with 1,3-Cyclic Diketones, Chin. J. Catal., 2012, 33, 1825-1831.
[21] Alizadeh A., Abdi G., Khodaei M.M., Ashokkumar M., Amirian J., Graphene oxide/Fe_3O_4/SO_3H nanohybrid: a new adsorbent for adsorption and reduction of Cr(VI) from aqueous solutions, RSC Adv., 2017, 7, 14876-14887.
[22] Kralj S., Drofenik M., Makovec D., Controlled surface functionalization of silica-coated magnetic nanoparticles with terminal amino and carboxyl groups, J. Nanopart. Res., 2011, 13, 2829-2841.
[23] Karaoglu E., Summak M.M., Baykal A., Sözeri H., Toprak M.S., Synthesis and Characterization of Catalytically Activity Fe_3O_4–3-Aminopropyl-triethoxysilane/Pd Nanocomposite, J. Inorg. Organomet. Polym., 2013, 23, 409-417.
[24] Li G., Jiang Y., Huang K., Ding P., Chen J., Preparation and properties of magnetic Fe_3O_4–chitosan nanoparticles, J. Alloys Compd., 2008, 466, 451-456.
[25] Naeimi H., Mohamadabadi S., Sulfonic acid-functionalized silica-coated magnetic nanoparticles as an efficient reusable catalyst for the synthesis of 1-substituted 1H-tetrazoles under solvent-free conditions, Dalton Trans., 2014, 43, 12967-12973.
[26] Veisi H., Mohammadi P., Gholami J., Sulfamic acid heterogenized on functionalized magnetic Fe_3O_4 nanoparticles with diaminoglyoxime as a green, efficient and reusable catalyst for one-pot synthesis of substituted pyrroles in aqueous phase, Appl. Organometal. Chem., 2014, 28, 868-873.
[27] Yamaura M., Camilo R.L., Sampaio L.C., Macedo M.A., Nakamura M., Toma H.E., Preparation and characterization of (3-aminopropyl) triethoxysilane-coated magnetite nanoparticles, J. Magn. Magn. Mater., 2004, 279, 210-217.
[28] Li J., Liang X., Magnetic solid acid catalyst for biodiesel synthesis from waste oil, Energy Convers. Manage., 2017, 141, 126-132.